



PAPER • OPEN ACCESS

Enhanced pair correlation functions in the two-dimensional Hubbard model

To cite this article: Takashi Yanagisawa 2013 *New J. Phys.* **15** 033012

View the [article online](#) for updates and enhancements.

You may also like

- [The analytic Bethe ansatz for a chain with centrally extended](#)

su(2|2)

[symmetry](#)

Niklas Beisert

- [How to read between the lines of electronic spectra: the diagnostics of fluctuations in strongly correlated electron systems](#)

Thomas Schäfer and Alessandro Toschi

- [Bethe equations for generalized Hubbard models](#)

Victor Fomin, Luc Frappat and Eric Ragoucy

Enhanced pair correlation functions in the two-dimensional Hubbard model

Takashi Yanagisawa

Electronics and Photonics Research Institute, National Institute of Advanced Industrial Science and Technology (AIST), Central 2, 1-1-1 Umezono, Tsukuba, Ibaraki 305-8568, Japan
E-mail: t-yanagisawa@aist.go.jp

New Journal of Physics **15** (2013) 033012 (14pp)

Received 11 October 2012

Published 11 March 2013

Online at <http://www.njp.org/>

doi:10.1088/1367-2630/15/3/033012

Abstract. In this study we have computed the pair correlation functions in the two-dimensional Hubbard model using a quantum Monte Carlo method. We employ a new diagonalization algorithm in the quantum Monte Carlo method which is free from the negative sign problem. We show that the d-wave pairing correlation function is indeed enhanced slightly for the positive on-site Coulomb interaction U when doping away from the half-filling. When the system size becomes large, the pair correlation function P_d increases for $U > 0$ compared to the non-interacting case, while P_d is suppressed for $U > 0$ when the system size is small. The enhancement ratio $P_d[U]/P_d[U = 0]$ will give a criterion on the existence of superconductivity. The ratio $P_d[U]/P_d[U = 0]$ increases almost linearly $\propto L$ when the system size $L \times L$ is increased. This increase is a good indication of the existence of a superconducting phase in the two-dimensional Hubbard model. There is, however, no enhancement of pair correlation functions in the half-filled case, which indicates the absence of superconductivity without hole doping.



Content from this work may be used under the terms of the [Creative Commons Attribution-NonCommercial-ShareAlike 3.0 licence](https://creativecommons.org/licenses/by-nc-sa/3.0/). Any further distribution of this work must maintain attribution to the author(s) and the title of the work, journal citation and DOI.

Contents

1. Introduction	2
2. The Model and the wave function	3
2.1. Hamiltonian	3
2.2. Quantum Monte Carlo (QMC) method—Metropolis algorithm	4
2.3. QMC method—diagonalization algorithm	5
3. Pair correlation functions	6
3.1. Comparison of the two methods	7
3.2. Pair correlation in the two-dimensional Hubbard model	8
4. Summary	11
Acknowledgments	13
References	13

1. Introduction

Strongly correlated electron systems have been studied intensively in relation to high-temperature superconductivity. High-temperature superconductors [1–4] are known to be a typical correlated electron system. In recent years, the mechanism of superconductivity in high-temperature superconductors has been extensively studied using various two-dimensional (2D) models of electronic interactions. Among them the 2D Hubbard model [5] is the simplest and most fundamental model. This model has been studied intensively using numerical tools, such as the quantum Monte Carlo (QMC) method [6–21] and the variational Monte Carlo (VMC) method [22–33].

The QMC method is a numerical method employed to simulate the behavior of correlated electron systems. It is well known, however, that there are significant issues associated with the application of the QMC method. The most important one is that the standard Metropolis (or heat bath) algorithm is associated with the negative sign problem. In past studies, workers have investigated the possibility of eliminating the negative sign problem [16, 17, 19, 21].

In this paper, we adopt an optimization scheme which is based on the diagonalization quantum Monte Carlo (QMD) method [21] (a bosonic version was developed in [34]), as well as the Metropolis quantum Monte Carlo method (called the Metropolis QMC in this paper). In general, and as in this study, the ground-state wave function is defined as

$$\psi = e^{-\tau H} \psi_0, \quad (1)$$

where H is the Hamiltonian and ψ_0 is the initial one-particle state such as the Fermi sea. In the QMD method this wave function is written as a linear combination of the basis states, generated using the auxiliary field method based on the Hubbard–Stratonovich transformation, that is,

$$\psi = \sum_m c_m \phi_m, \quad (2)$$

where ϕ_m are basis functions. In this work, we have assumed a subspace with N_{states} basis wave functions. From the variational principle, the coefficients $\{c_m\}$ are determined from the diagonalization of the Hamiltonian, to obtain the lowest energy state in the selected

subspace $\{\phi_m\}$. Once the c_m coefficients are determined, the ground-state energy and other quantities are calculated using this wave function. If the expectation values are not highly sensitive to the number of basis states, we can obtain the correct expectation values using an extrapolation in terms of the basis states in the limit $N_{\text{states}} \rightarrow \infty$.

Whether the 2D Hubbard model can account for high-temperature superconductivity is an important question in the study of high-temperature superconductors. In correlated electron systems, there is an interesting phenomenological correlation between the maximum T_c and the transfer integral t :

$$k_B T_c \simeq 0.1t/(m^*/m), \quad (3)$$

where m^*/m indicates the mass enhancement factor and $t_{\text{eff}} \equiv t/(m^*/m)$ is the effective transfer integral. By adopting $t \sim 0.5$ eV [35] and $m^*/m \sim 5$, this formula applies to high- T_c cuprates with $T_c \sim 100$ K. As the electron becomes heavier, T_c is lowered (in accordance with the lowering of T_c in the underdoped region). We can choose $t \sim 0.1$ eV and $m^*/m \sim 2$ for iron pnictides to give $T_c \sim 50$ K. This formula strongly suggests that high-temperature superconductivity originates from the electron correlation and not from the electron–phonon interaction.

Most of the QMC method results do not support superconductivity, although the results of the VMC method with the Gutzwiller ansatz indicate the stable d-wave pairing state for large U . The computations of the pair-field susceptibility suggest the existence of the Kosterlitz–Thouless transition in the 2D Hubbard model indicating superconducting transition in real three-dimensional systems [36, 37]. The perturbative and random phase approximation (RPA) calculations also support superconductivity with anisotropic pairing symmetry [38–42]. In contrast, the pair correlation functions obtained by a QMC method [18] are extremely suppressed for the intermediate values of U . This result suggests that superconductivity is impossible in the 2D Hubbard model. The objective of this paper is to compute pair correlation functions and clarify this discrepancy using a new QMC method by employing the diagonalization scheme [21]. We show that the pair correlation function is indeed enhanced at doping.

2. The Model and the wave function

2.1. Hamiltonian

The Hamiltonian is the Hubbard model containing on-site Coulomb repulsion and is written as

$$H = - \sum_{ij\sigma} t_{ij} (c_{i\sigma}^\dagger c_{j\sigma} + \text{h.c.}) + U \sum_j n_{j\uparrow} n_{j\downarrow}, \quad (4)$$

where $c_{j\sigma}^\dagger$ ($c_{j\sigma}$) is the creation (annihilation) operator of an electron with spin σ at the j th site and $n_{j\sigma} = c_{j\sigma}^\dagger c_{j\sigma}$. Note that t_{ij} is the transfer energy between the sites i and j . $t_{ij} = t$ for the nearest-neighbor bonds and $t_{ij} = -t'$ for the next-nearest-neighbor bonds. For all other cases $t_{ij} = 0$. U is the on-site Coulomb energy. The number of sites is N and the linear dimension of the system is denoted as L , i.e. $N = L^2$. The energy unit is given by t and the number of electrons is denoted as N_e .

2.2. Quantum Monte Carlo (QMC) method—Metropolis algorithm

In a QMC simulation, the ground-state wave function is

$$\psi = e^{-\tau H} \psi_0, \quad (5)$$

where ψ_0 is the initial one-particle state represented by a Slater determinant. For large τ , $e^{-\tau H}$ will project out the ground state from ψ_0 . We write the Hamiltonian as $H = K + V$, where K and V are the kinetic and interaction terms of the Hamiltonian in equation (4), respectively. The wave function in equation (5) is written as

$$\psi = (e^{-\Delta\tau(K+V)})^m \psi_0 \approx (e^{-\Delta\tau K} e^{-\Delta\tau V})^m \psi_0 \quad (6)$$

for $\tau = \Delta\tau m$. Using the Hubbard–Stratonovich transformation [6, 43], we have

$$\exp(-\Delta\tau U n_{i\uparrow} n_{i\downarrow}) = \frac{1}{2} \sum_{s_i = \pm 1} \exp(2as_i(n_{i\uparrow} - n_{i\downarrow}) - \frac{1}{2}U\Delta\tau(n_{i\uparrow} + n_{i\downarrow})) \quad (7)$$

for $(\tanh a)^2 = \tanh(\Delta\tau U/4)$ or $\cosh(2a) = e^{\Delta\tau U/2}$. The wave function is expressed as a summation of the one-particle Slater determinants over all the configurations of the auxiliary fields $s_j = \pm 1$. The exponential operator is expressed as [43]

$$(e^{-\Delta\tau K} e^{-\Delta\tau V})^m = \frac{1}{2^{Nm}} \sum_{\{s_i(\ell)\}} \prod_{\sigma} B_m^{\sigma}(s_i(m)) B_{m-1}^{\sigma}(s_i(m-1)) \cdots B_1^{\sigma}(s_i(1)), \quad (8)$$

where we have defined

$$B_{\ell}^{\sigma}(\{s_i(\ell)\}) = e^{-\Delta\tau K_{\sigma}} e^{-V_{\sigma}(\{s_i(\ell)\})} \quad (9)$$

for

$$V_{\sigma}(\{s_i\}) = 2a\sigma \sum_i s_i n_{i\sigma} - \frac{1}{2}U\Delta\tau \sum_i n_{i\sigma}, \quad (10)$$

$$K_{\sigma} = - \sum_{ij} t_{ij} (c_{i\sigma}^{\dagger} c_{j\sigma} + \text{h.c.}). \quad (11)$$

The ground-state wave function is

$$\psi = \sum_n c_n \phi_n, \quad (12)$$

where ϕ_n is a Slater determinant corresponding to a configuration $\{s_i(\ell)\}$ ($i = 1, \dots, N$; $\ell = 1, \dots, m$) of the auxiliary fields:

$$\begin{aligned} \phi_n &= \prod_{\sigma} B_m^{\sigma}(s_i(m)) \cdots B_1^{\sigma}(s_i(1)) \psi_0 \\ &\equiv \phi_n^{\uparrow} \phi_n^{\downarrow}. \end{aligned} \quad (13)$$

The coefficients c_n are constant real numbers: $c_1 = c_2 = \cdots$. The initial state ψ_0 is a one-particle state. The matrix of $V_{\sigma}(\{s_i\})$ is a diagonal matrix given as

$$V_{\sigma}(\{s_i\}) = \text{diag}(2a\sigma s_1 - U\Delta\tau/2, \dots, 2a\sigma s_N - U\Delta\tau/2). \quad (14)$$

The matrix elements of K_σ are

$$(K_\sigma)_{ij} = \begin{cases} -t, & i, j \text{ are nearest neighbors,} \\ 0, & \text{otherwise.} \end{cases} \quad (15)$$

ϕ_n^σ is an $N \times N_\sigma$ matrix given by the product of the matrices $e^{-\Delta\tau K_\sigma}$, e^{V_σ} and ψ_0^σ . The inner product is thereby calculated as a determinant [17],

$$\langle \phi_\ell^\sigma \phi_n^\sigma \rangle = \det(\phi_\ell^{\sigma\dagger} \phi_n^\sigma). \quad (16)$$

The expectation value of the quantity Q is evaluated as

$$\langle Q \rangle = \frac{\sum_{\ell n} \langle \phi_\ell Q \phi_n \rangle}{\sum_{\ell n} \langle \phi_\ell \phi_n \rangle}. \quad (17)$$

$P_{\ell n} \equiv \det(\phi_\ell^\sigma \phi_n^\sigma) \det(\phi_\ell^{-\sigma} \phi_n^{-\sigma})$ can be regarded as the weighting factor to obtain the Monte Carlo samples. Since this quantity is not necessarily positive definite, the weighting factor should be $|P_{\ell n}|$; the resulting relationship is

$$\begin{aligned} \langle Q_\sigma \rangle &= \sum_{\ell n} P_{\ell n} \langle Q_\sigma \rangle_{\ell n} / \sum_{\ell n} P_{\ell n} \\ &= \sum_{\ell n} |P_{\ell n}| \text{sign}(P_{\ell n}) \langle Q_\sigma \rangle_{\ell n} / \sum_{\ell n} |P_{\ell n}| \text{sign}(P_{\ell n}), \end{aligned} \quad (18)$$

where $\text{sign}(a) = a/|a|$ and

$$\langle Q_\sigma \rangle_{\ell n} = \frac{\langle \phi_\ell^\sigma Q_\sigma \phi_n^\sigma \rangle}{\langle \phi_\ell^\sigma \phi_n^\sigma \rangle}. \quad (19)$$

This relation can be evaluated using a Monte Carlo procedure if an appropriate algorithm, such as the Metropolis or heat bath method, is employed [43]. The summation can be evaluated using appropriately defined Monte Carlo samples,

$$\langle Q_\sigma \rangle = \frac{\frac{1}{n_{\text{MC}}} \sum_{\ell n} \text{sign}(P_{\ell n}) \langle Q_\sigma \rangle_{\ell n}}{\frac{1}{n_{\text{MC}}} \sum_{mn} \text{sign}(P_{\ell n})}, \quad (20)$$

where n_{MC} is the number of samples. The sign problem is an issue if the summation of $\text{sign}(P_{\ell n})$ vanishes within statistical errors. In this case, it is indeed impossible to obtain definite expectation values.

2.3. QMC method—diagonalization algorithm

Quantum Monte Carlo diagonalization (QMD) is a method for the evaluation of $\langle Q_\sigma \rangle$ without the negative sign problem. The configuration space of the probability $\|P_{mn}\|$ in equation (20) is generally very strongly peaked. The sign problem lies in the distribution of P_{mn} in the configuration space. It is important to note that the distribution of the basis functions ϕ_m ($m = 1, 2, \dots$) is uniform since c_m are constant numbers: $c_1 = c_2 = \dots$. In the subspace $\{\phi_m\}$, selected from all configurations of auxiliary fields, the right-hand side of equation (17) can be determined. However, the large number of basis states required to obtain accurate expectation

values is beyond the current storage capacity of computers. Thus, we use the variational principle to obtain the expectation values.

From the variational principle,

$$\langle Q \rangle = \frac{\sum_{mn} c_m c_n \langle \phi_m Q \phi_n \rangle}{\sum_{mn} c_m c_n \langle \phi_m \phi_n \rangle}, \quad (21)$$

where c_m ($m = 1, 2, \dots$) are variational parameters. In order to minimize the energy

$$E = \frac{\sum_{mn} c_m c_n \langle \phi_m H \phi_n \rangle}{\sum_{mn} c_m c_n \langle \phi_m \phi_n \rangle} \quad (22)$$

the equation $\partial E / \partial c_n = 0$ ($n = 1, 2, \dots$) is solved for,

$$\sum_m c_m \langle \phi_n H \phi_m \rangle - E \sum_m c_m \langle \phi_n \phi_m \rangle = 0. \quad (23)$$

If we set

$$H_{mn} = \langle \phi_m H \phi_n \rangle, \quad (24)$$

$$A_{mn} = \langle \phi_m \phi_n \rangle \quad (25)$$

the eigenequation is

$$Hu = EAu \quad (26)$$

for $u = (c_1, c_2, \dots)^t$. Since ϕ_m ($m = 1, 2, \dots$) are not necessarily orthogonal, A is not a diagonal matrix. We diagonalize the Hamiltonian $A^{-1}H$ and then calculate the expectation values of correlation functions with the ground state eigenvector; in general $A^{-1}H$ is not a symmetric matrix.

In order to optimize the wave function, we must increase the number of basis states $\{\phi_m\}$. This can be simply accomplished through random sampling. For systems of small sizes and small U , we can evaluate the expectation values from an extrapolation of the basis of randomly generated states. The number of basis states is about 2000 when the system size is small. For systems 8×8 and 10×10 , the number of states is increased up to about 10 000.

In QMC simulations an extrapolation is performed to obtain the expectation values for the ground-state wave function. The variance method has been proposed in variational and QMC simulations, where the extrapolation is performed as a function of the variance. An advantage of the variance method is that linearity is expected in some cases [19, 44]:

$$\langle Q \rangle - Q_{\text{exact}} \propto v, \quad (27)$$

where v denotes the variance defined as

$$v = \frac{\langle (H - \langle H \rangle)^2 \rangle}{\langle H \rangle^2} \quad (28)$$

and Q_{exact} is the expected exact value of the quantity Q .

3. Pair correlation functions

In this section, we present the results obtained by the QMC and QMD methods.

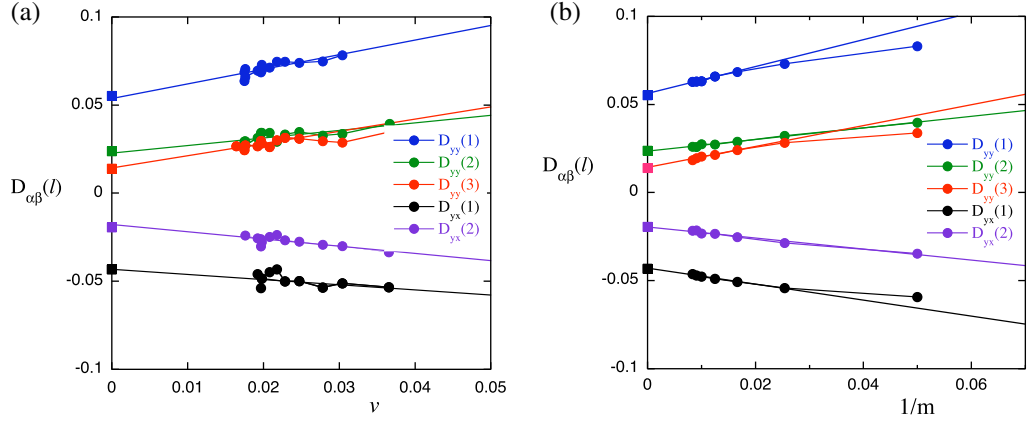


Figure 1. Pair correlation functions $D_{yy}(\ell)$ and $D_{yx}(\ell)$ for 4×3 , $U = 4$ and $N_e = 10$ obtained by the diagonalization QMC method (a) and the Metropolis QMC method (b). The squares are the exact results obtained by the exact diagonalization method. In (a) the data fit using a straight line using the least-square method as the variance is reduced. We started with $N_{\text{states}} = 100$ (the first solid circles) and then increase up to 2000.

3.1. Comparison of the two methods

The pair correlation function $D_{\alpha\beta}$ is defined by

$$D_{\alpha\beta}(\ell) = \langle \Delta_{\alpha}^{\dagger}(i + \ell) \Delta_{\beta}(i) \rangle, \quad (29)$$

where $\Delta_{\alpha}(i)$, $\alpha = x, y$, denote the annihilation operators of the singlet electron pairs for the nearest-neighbor sites:

$$\Delta_{\alpha}(i) = c_{i\downarrow}c_{i+\hat{\alpha}\uparrow} - c_{i\uparrow}c_{i+\hat{\alpha}\downarrow}. \quad (30)$$

Here $\hat{\alpha}$ is a unit vector in the $\alpha(=x, y)$ -direction. We consider the correlation function of d-wave pairing:

$$P_d(\ell) = \langle \Delta_d(i + \ell)^{\dagger} \Delta_d(i) \rangle, \quad (31)$$

where

$$\Delta_d(i) = \Delta_x(i) + \Delta_{-x}(i) - \Delta_y(i) - \Delta_{-y}(i), \quad (32)$$

i and $i + \ell$ denote sites on the lattice.

We show how the pair correlation function is evaluated in QMC methods. We show the pair correlation functions D_{yy} and D_{yx} on the lattice 4×3 in figure 1. The boundary condition is open in the four-site direction and is periodic in the other direction. An extrapolation is performed as a function of $1/m$ in the QMC method with Metropolis algorithm and as a function of the energy variance v in the QMD method with diagonalization. We keep $\Delta\tau$ a small constant $\simeq 0.02$ – 0.05 and increase $\tau = \Delta\tau m$, where m is the division number m of the wave function ψ in equation (5). In the Metropolis QMC method, we calculated averages over 5×10^5 Monte Carlo steps. The exact values were obtained by using the exact diagonalization method. The two methods give consistent results as shown in the figures. All the $D_{yy}(\ell)$ and

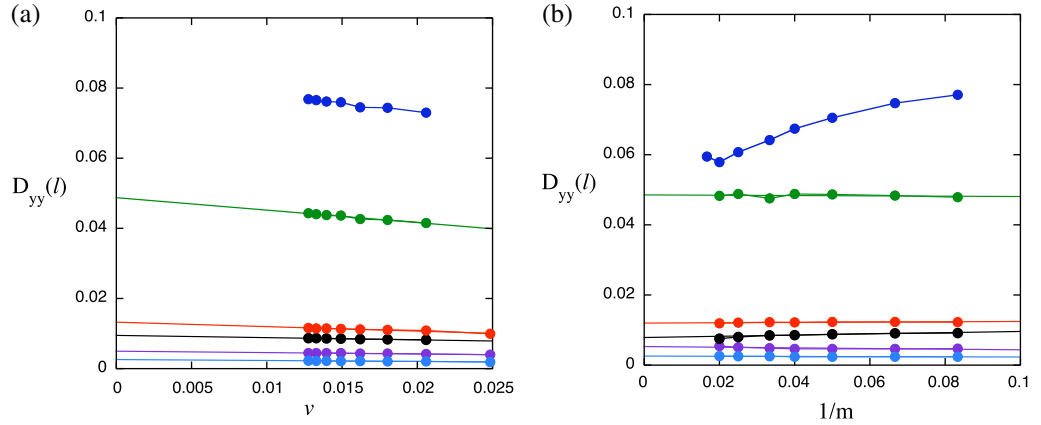


Figure 2. Pair correlation function $D_{yy}(\ell)$ as a function of the energy variance v in (a) and $1/m$ in (b) for 30×2 , $U = 4$ and $N_e = 48$. We used (a) the diagonalization QMC method and (b) the Metropolis QMC method. We set the open boundary condition. From the top, $\ell = (1, 0)$, $(2, 0)$, $(5, 0)$, $(4, 0)$, $(3, 0)$ and $(6, 0)$.

$D_{yx}(\ell)$ are suppressed on 4×3 when U is increased. In general, the pair correlation functions are suppressed in small systems.

In figure 2, we show the inter-chain pair correlation function $D_{yy}(\ell)$ as a function of $1/m$ (b) and the energy variance (a) for the ladder model 30×2 . We use the open boundary condition. The boundary condition is not important for our purpose to check the consistency between QMC and QMD methods. The number of electrons is $N_e = 48$, and the strength of the Coulomb interaction is $U = 4$. $\Delta_y(i)$ indicates the electron pair along the rung, and $D_{yy}(\ell)$ is the expectation value of the parallel movement of the pair along the ladder. The results obtained by the two methods are in good agreement except for $\ell = (1, 0)$ (nearest-neighbor correlation).

3.2. Pair correlation in the two-dimensional Hubbard model

We present the results for pair correlation in the 2D Hubbard model. In this section, we show the results using the diagonalization QMC method because the Metropolis QMC method has a negative sign problem. We first examine the 8×8 lattice. The P_d was estimated by an extrapolation as a function of the variance v , as shown in figure 3, where the computations were carried out on an 8×8 lattice with $U = 3$, $t' = -0.2$ and $N_e = 54$. The extrapolation was successfully performed for 8×8 .

We consider the half-filled case with $t' = 0$; in this case the antiferromagnetic correlation is dominant over the superconductive pairing correlation and thus the pairing correlation function is suppressed as the Coulomb repulsion U is increased. Figure 4(a) exhibits the d-wave pairing correlation function P_d on an 8×8 lattice as a function of the distance. The P_d is suppressed due to the on-site Coulomb interaction, as expected. Its reduction is, however, not so considerably large compared to previous QMC studies [18] where the pairing correlation is almost annihilated for $U = 4$. We then turn to the case of less than half-filling. We show the results on 8×8 with electron number $N_e = 54$. We show P_d as a function of the distance in figure 4(b) ($N_e = 54$). In the scale of this figure, P_d for $U > 0$ is almost the same as that of the non-interacting case, and is

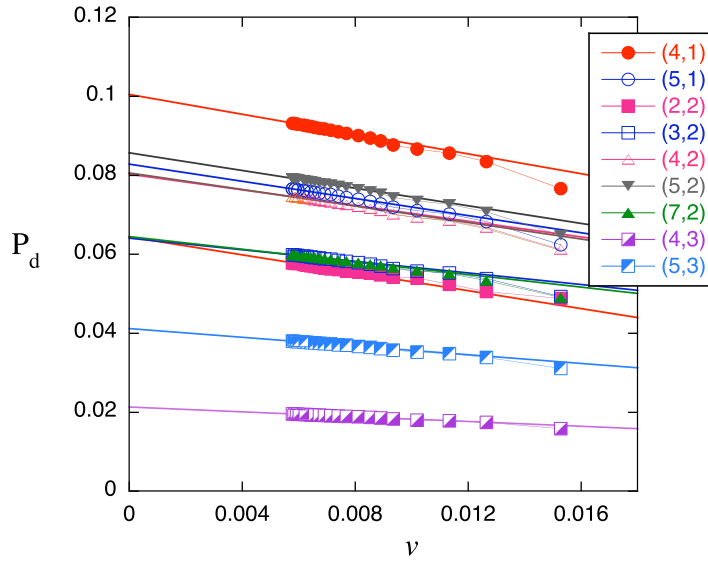


Figure 3. Pair correlation function P_d as a function of the energy variance v on an 8×8 lattice. $U = 3$, $t' = -0.2$ and the electron number is $N_e = 54$. We have shown $P_d(\ell) = \langle \Delta_d(i + \ell)^\dagger \Delta(i) \rangle$ for $\ell = (m, n) - i$ and $i = (1, 1)$, where (m, n) are shown in the figure.

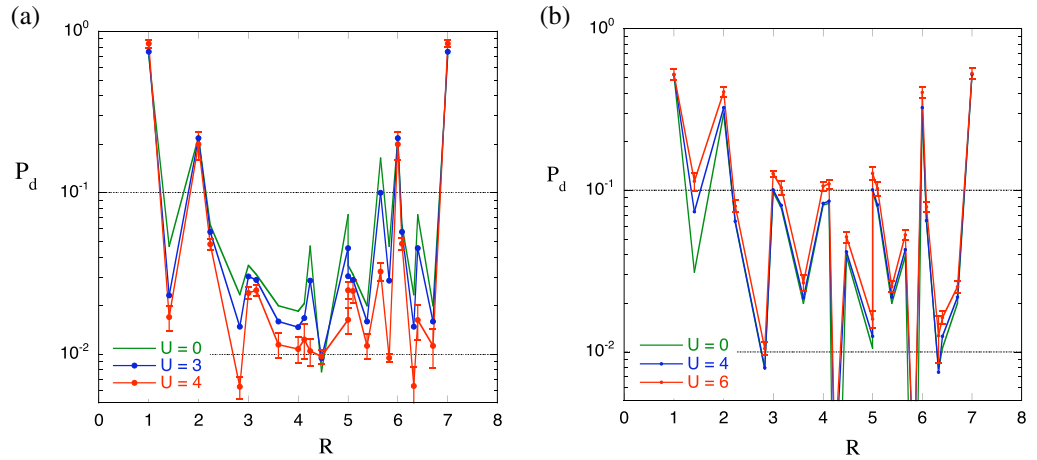


Figure 4. Pair correlation function P_d as a function of the distance $R = |\ell|$ on an 8×8 lattice for (a) the half-filled case $N_e = 64$ and (b) $N_e = 54$. We set $t' = 0.0$ and $U = 0, 3$ and 4 for (a) and $t' = -0.2$ and $U = 0, 4$ and 6 for (b). To lift the degeneracy of electron configurations at the Fermi energy in the half-filled case, we included a small staggered magnetization $\sim 10^{-4}$ in the initial wave function ψ_0 .

enhanced slightly for large U . Our results indicate that the pairing correlation is not suppressed and is indeed enhanced by the Coulomb interaction U , and its enhancement is very small. Figure 5 represents P_d as a function of U for $N_e = 54, 50$ and 64 . We set $t' = 0$ for $N_e = 50$ and $t' = -0.2$ for $N_e = 54$ so that we have the closed shell structure in the initial function. In the system of this size, the effect of the inclusion of $t' \neq 0$ is small. Figure 6 shows P_d on a

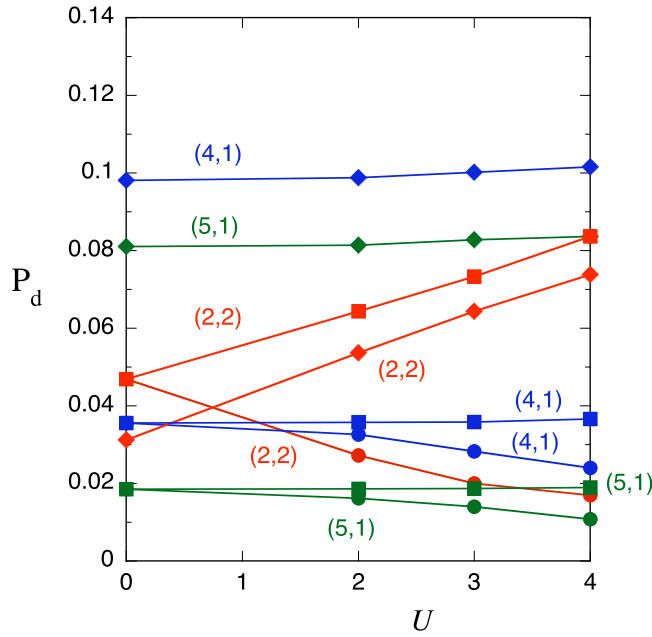


Figure 5. Pair correlation function P_d as a function of U on an 8×8 lattice. $t' = -0.2$ for $N_e = 54$ (diamonds), and $t' = 0$ for $N_e = 50$ (squares) and $N_e = 64$ (circles). We have shown $P_d(\ell) = \langle \Delta_d(i + \ell)^\dagger \Delta(i) \rangle$ for $\ell = (m, n) - i$ and $i = (1, 1)$, where (m, n) are shown in the figure.

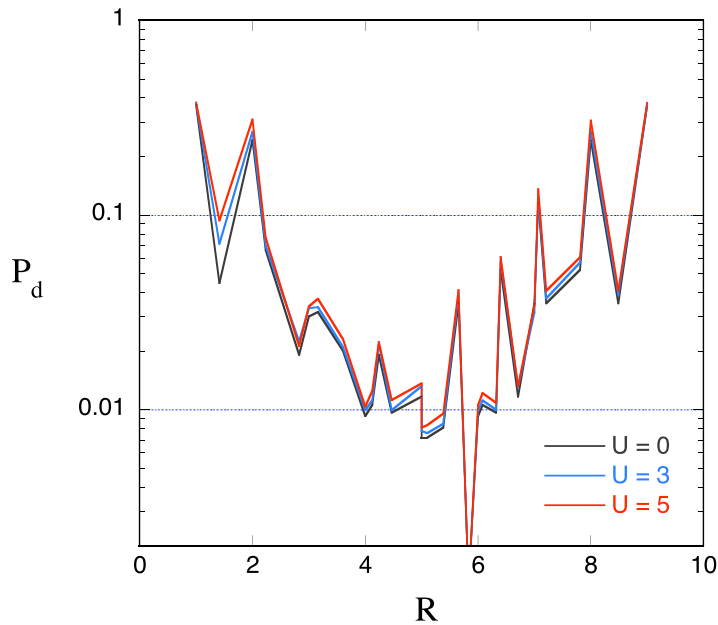


Figure 6. Pair correlation function P_d as a function of the distance $R = |\ell|$ on a 10×10 lattice for $N_e = 82$ and $t' = -0.2$. The strength of the Coulomb interaction is $U = 0, 3$ and 5 .

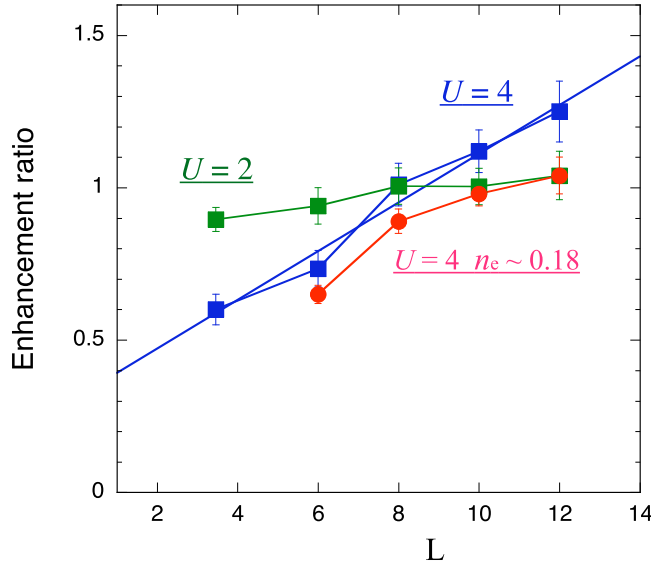


Figure 7. Enhancement ratio of the pair correlation function $P_d|_U/P_d|_{U=0}$ as a function of the linear system size L for $U = 4$ and 2 . The electron density n_e is about 0.8 : $n_e \sim 0.8$ for squares. The data for $U = 4$ and $n_e \sim 0.18$ are also shown by circles.

10×10 lattice. This also indicates that the pairing correlation function is enhanced for $U > 0$. There is a tendency that P_d is easily suppressed as the system size becomes small. We estimated the enhancement ratio compared to the non-interacting case $P_d(\ell)|_U/P_d(\ell)|_{U=0}$ at $|\ell| \sim L/2$ for $n_e \sim 0.8$ as shown in figure 7. This ratio increases as when system size is increased. To compute the enhancement, we picked the sites, for example on an 8×8 lattice, $\ell = (3, 2), (4, 0), (4, 1), (3, 3), (4, 2), (4, 3), (5, 0), (5, 1)$ with $|\ell| \sim 4-5$ and evaluate the mean value. In our computations, the ratio increases almost linearly, indicating a possibility of superconductivity. This indicates $P_d(\ell) \sim LP_d(\ell) \sim \ell P_d(\ell)$ for $\ell \sim L$. Because $P_d(\ell)|_{U=0} \sim 1/|\ell|^3$, we obtain $P_d(\ell) \sim \ell P_d(\ell) \sim 1/|\ell|^2$ for $|\ell| \sim L$. This indicates that the exponent of the power law is 2. When $U = 2$, the enhancement is small and is almost independent of L . In the low-density case, the enhancement is also suppressed being equal to 1. In figure 8, the enhancement ratio is shown as a function of the electron density n_e for $U = 4$. A dome structure emerges even in small systems. The square in figure 8 indicates the result for the half-filled case with $t' = -0.2$ on an 8×8 lattice. This is the open shell case and causes difficulty in computations as a result of the degeneracy due to partially occupied electrons. The inclusion of $t' < 0$ enhances P_d compared to the case with $t' = 0$ on an 8×8 lattice. P_d is, however, not enhanced over the non-interacting case at half-filling. This also holds for a 10×10 lattice where the enhancement ratio ~ 1 . This indicates the absence of superconductivity at half-filling.

4. Summary

The quest for the existence of superconducting transition in the 2D Hubbard model remains unresolved. Pair correlation functions had been calculated by using QMC methods, and their results were negative for the existence of superconductivity in many works. The objective of this paper was to reexamine this question by elaborating a sampling method of the QMC method.

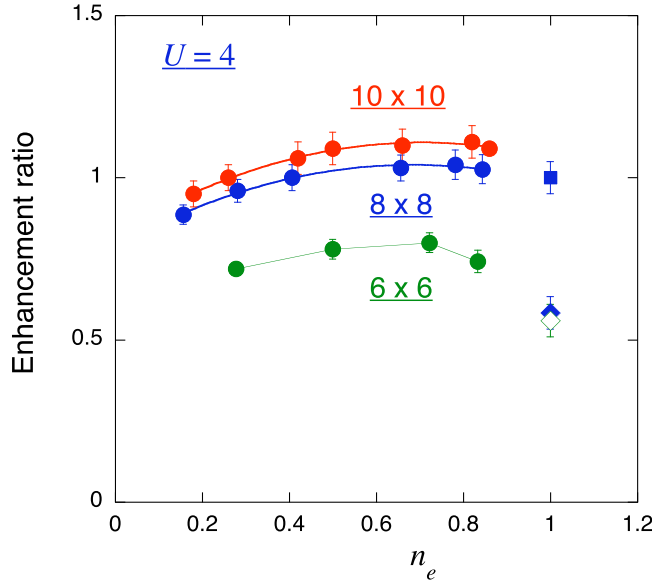


Figure 8. Enhancement ratio of the pair correlation function $P_d|_U/P_d|_{U=0}$ as a function of the electron density n_e . We adopt $t' = -0.2$ and $U = 4$. For the half-filled case, the diamonds are for $t' = 0$ on an 8×8 lattice (solid diamond) and a 6×6 lattice (open diamond). The square is for $t' = -0.2$ on 8×8 and 10×10 where there is no enhancement.

We have calculated the d-wave pair correlation function P_d for the 2D Hubbard model by using the QMC method. In the half-filled case P_d is suppressed for the repulsive $U > 0$, and when doped away from half-filling $N_e < N$, P_d is enhanced slightly for $U > 0$. It is noteworthy that the correlation function P_d is indeed enhanced and increases as the system size increases in the 2D Hubbard model. The enhancement ratio increases almost linearly $\propto L$ when the system size is increased, which is indicative of the existence of superconductivity. Our criterion is that when the enhancement ratio as a function of the system size L is proportional to a certain power of L , superconductivity will be developed. This ratio depends on U and is reduced when U is decreased. The dependence on the band filling shows a dome structure as a function of the electron density. In the 10×10 system, the ratio is greater than 1 in the range $0.3 < n_e < 0.9$. This does not immediately indicate the existence of superconductivity. The size dependence is important and is needed to obtain the doping range where superconductivity exists. Let us also mention the superconductivity at half-filling. Our results indicate the absence of superconductivity in the half-filling case because there is no enhancement of pair correlation functions. This is consistent with the results for an anisotropic triangular lattice [45].

We have compared two methods: diagonalization QMC and Metropolis QMC. For small systems, the results obtained by two methods are quite consistent. When the system size is large, $P_d(\ell)$ is inevitably suppressed and almost vanishes if we use the Metropolis QMC method. $P_d(\ell)$ decreases as the division number m increases in this method. We wonder whether this excessive suppression of $P_d(\ell)$ is true. In fact, the correlation function D_{yy} for the ladder Hubbard model obtained by the Metropolis QMC also shows a similar behavior when the size is increased, in contrast to the enhanced D_{yy} indicated by the density-matrix renormalization (DMRG) method [46]. The results of the diagonalization QMC are consistent with those of DMRG [21]. There is a possibility that this has some relation with the negative sign.

Acknowledgments

We thank J Kondo, K Yamaji, I Hase and S Koikegami for helpful discussions. This work was supported by a Grant-in-Aid for Scientific Research from the Ministry of Education, Culture, Sports, Science and Technology, Japan. This work was also supported by the CREST program of the Japan Science and Technology Agency (JST). Part of the numerical calculations was performed at the facilities in the Supercomputer Center of the Institute for Solid State Physics, University of Tokyo.

References

- [1] Dagotto E 1994 *Rev. Mod. Phys.* **66** 763
- [2] Scalapino D J 1990 *Proc. on The Los Alamos Symp. High Temperature Superconductivity (1989)* ed K S Bedell, D Coffey, D E Deltzer, D Pines and J R Schrieffer (Redwood City: Addison-Wesley) p 314
- [3] Anderson P W 1997 *The Theory of Superconductivity in the High- T_c Cuprates* (Princeton, NJ: Princeton University Press)
- [4] Moriya T and Ueda K 2000 *Adv. Phys.* **49** 555
- [5] Hubbard J 1963 *Proc. R. Soc. Lond. A* **276** 238
- [6] Hirsch J E 1983 *Phys. Rev. Lett.* **51** 1900
- [7] Hirsch J E 1985 *Phys. Rev. B* **31** 4403
- [8] Sorella S, Tosatti E, Baroni S, Car R and Parrinell M 1988 *Int. J. Mod. Phys. B* **2** 993
- [9] White S R, Scalapino D J, Sugar R L, Loh E Y, Gubernatis J E and Scalettar R T 1989 *Phys. Rev. B* **40** 506
- [10] Imada M and Hatsugai Y 1989 *J. Phys. Soc. Japan* **58** 3752
- [11] Sorella S, Baroni S, Car R and Parrinello M 1989 *Europhys. Lett.* **8** 663
- [12] Loh E Y, Gubernatis J E, Scalettar R T, White S R, Scalapino D J and Sugar R L 1990 *Phys. Rev. B* **41** 9301
- [13] Moreo A, Scalapino D J and Dagotto E 1991 *Phys. Rev. B* **56** 11442
- [14] Furukawa N and Imada M 1992 *J. Phys. Soc. Japan* **61** 3331
- [15] Moreo A 1992 *Phys. Rev. B* **45** 5059
- [16] Fahy S and Hamann D R 1991 *Phys. Rev. B* **43** 765
- [17] Zhang S, Carlson J and Gubernatis J E 1997 *Phys. Rev. B* **55** 7464
- [18] Zhang S, Carlson J and Gubernatis J E 1997 *Phys. Rev. Lett.* **78** 4486
- [19] Kashima T and Imada M 2001 *J. Phys. Soc. Japan* **70** 2287
- [20] Yanagisawa T, Koike S and Yamaji K 1998 *J. Phys. Soc. Japan* **67** 3867
- [21] Yanagisawa T 2007 *Phys. Rev. B* **75** 224503
- [22] Yokoyama H and Shiba H 1987 *J. Phys. Soc. Japan* **56** 1490
Yokoyama H and Shiba H 1987 *J. Phys. Soc. Japan* **56** 3582
- [23] Gros C, Joynt R and Rice T M 1987 *Phys. Rev. B* **36** 381
- [24] Nakanishi T, Yamaji K and Yanagisawa T 1997 *J. Phys. Soc. Japan* **66** 294
- [25] Yamaji K, Yanagisawa T, Nakanishi T and Koike S 1998 *Physica C* **304** 225
Yamaji K, Yanagisawa T, Nakanishi T and Koike S 2000 *Physica B* **284** 415
- [26] Koike S, Yamaji K and Yanagisawa T 1999 *J. Phys. Soc. Japan* **68** 1657
Koike S, Yamaji K and Yanagisawa T 2000 *J. Phys. Soc. Japan* **69** 2199
- [27] Yanagisawa T, Koike S and Yamaji K 2001 *Phys. Rev. B* **64** 184509
- [28] Yanagisawa T, Koike S and Yamaji K 2002 *J. Phys.: Condens. Matter* **14** 21
- [29] Yanagisawa T, Miyazaki M, Koikegami S, Koike S and Yamaji K 2003 *Phys. Rev. B* **67** 132408
- [30] Yanagisawa T, Miyazaki M and Yamaji K 2009 *J. Phys. Soc. Japan* **78** 013706
- [31] Miyazaki M, Yamaji K and Yanagisawa T 2004 *J. Phys. Soc. Japan* **73** 1643
- [32] Tocchio L T, Becca F and Gros C 2011 *Phys. Rev. B* **83** 195138
- [33] Yokoyama H, Ogata M, Tanaka Y, Kobayashi K and Tsuchiura H 2013 *J. Phys. Soc. Japan* **82** 014707

- [34] Mizusaki T, Honma M and Otsuka T 1986 *Phys. Rev. C* **53** 2786
- [35] Feiner L F, Jefferson J H and Raimondi R 1996 *Phys. Rev. B* **53** 8751
- [36] Maier T A, Jarrell M, Schulthess T C, Kent P R C and White J B 2005 *Phys. Rev. Lett.* **95** 237001
- [37] Yanagisawa T 2010 *J. Phys. Soc. Japan* **79** 063708
- [38] Scalapino D J, Loh E and Hirsch J E 1986 *Phys. Rev. B* **34** 8190
- [39] Bickers N E, Scalapino D J and White S R 1989 *Phys. Rev. Lett.* **62** 961
- [40] Hlubina R 1999 *Phys. Rev. B* **59** 9600
- [41] Kondo J 2001 *J. Phys. Soc. Japan* **70** 808
- [42] Yanagisawa T 2008 *New J. Phys.* **10** 023014
- [43] Blankenbecler R, Scalapino D J and Sugar R L 1981 *Phys. Rev. D* **24** 2278
- [44] Sorella S 2001 *Phys. Rev. B* **64** 024512
- [45] Clay R T, Li H and Mazumdar S 2008 *Phys. Rev. Lett.* **101** 166403
- [46] Noack R M, Bulut N, Scalapino D J and Zacher M G 1997 *Phys. Rev. B* **56** 7162